Capacitance Properties of Graphite Oxide/Poly(3,4-ethylene dioxythiophene) Composites

Yongqin Han, Bing Ding, Hao Tong, Xiaogang Zhang

College of Material Science and Engineering, Nanjing University of Aeronautics and Astronautics, Nanjing 210016, China

Received 14 April 2010; accepted 13 October 2010
DOI 10.1002/app.33610
Published online 25 February 2011 in Wiley Online Library (wileyonlinelibrary.com).

ABSTRACT: Poly(3,4-ethylene dioxythiophene) (PEDOT) and graphite oxide (GO)/PEDOT composites (GPTs) doped with poly(sodium styrene sulfate) (PSS) were synthesized by *in situ* polymerization in aqueous media. The electrochemical capacitance performances of GO, PEDOT–PSS, and GPTs as electrode materials were investigated. The GPTs had a higher specific capacitance of 108 F/g than either composite constituent (11 F/g for GO and 87 F/g for PEDOT–PSS); this was attributable to its high electrical conductivity and the layer-within/on-layer composite structure. Such an increase demonstrated that the synergistic combination of GO and PEDOT–PSS had advantages over the sum of the individual components. On the basis of cycle-life tests, the capacitance retention of about 78% for the GPTs compared with that of 66% for PEDOT–PSS after 1200 cycles suggested a high cycle stability of the GPTs and its potential as an electrode material for supercapacitor applications. © 2011 Wiley Periodicals, Inc. J Appl Polym Sci 121: 892–898, 2011

Key words: composites; conducting polymers; electrochemistry

INTRODUCTION

Digital communications, electric vehicles, and other devices that require electrical energy at high power levels in relatively short pulses have prompted considerable research on supercapacitors. Supercapacitors can be divided into two categories on the basis of their charge-storage mechanism: electrical double-layer capacitors (EDLCs) and redox supercapacitors. Energy storage in an EDLC is due to the charging of the electrical double layer at the electrode–electrolyte interface; however, a redox supercapacitor uses faradic reactions in addition to the double-layer charge.[1–4] The main materials used for supercapacitor electrode preparation include carbon materials, such as activated carbon, carbon nanotubes, and activated carbon fibers,[5–8] and electroactive materials with several redox states or structures, such as transition-metal oxides (e.g., oxides of ruthenium, nickel, cobalt, indium, tin, and manganese)[9–12] and conducting polymers.[13–16]

The high cost and/or toxic characteristics of intensively studied inorganic supercapacitor electrode materials, such as carbon nanotubes and RuO_2, have limited their application as supercapacitor electrodes. Nowadays, most research on supercapacitors aims to increase the electrochemical performance and lower the fabrication costs and to simultaneously use environmentally friendly materials. Graphite oxide (GO), with a low fabrication cost and an environmentally friendly nature, can be obtained on a large scale by the chemical oxidation of graphite, and it possesses a number of hydroxyl and epoxide functional groups anchored on sp^3-hybridized carbon atoms on both surfaces of each sheet and considerable amounts of sp^2-hybridized carbon-atom-containing carboxyl and carbonyl groups at the sheet edges.[17–20] Unfortunately, the functional groups and poor electrical conductivity resulting from the oxidation of the graphite can be obstacles for electrolyte motion between the graphene sheets. As a result, pristine GO, mainly possessing electric double-layer capacitance, provides a low specific capacitance (<30 F/g).[21] To improve the electrochemical performance of pristine GO, poly(sodium styrene sulfate) (PSS)[22] and poly(ethylene oxide)-*co*-poly(propylene oxide)[23] have been incorporated into GO to form composites, and these have shown improvements in the specific capacitance.

Conducting polymers have also been regarded as alternative electrode materials for electrochemical supercapacitors because of their pseudocapacitive

Correspondence to: X. Zhang (azhangxg@163.com).
Contract grant sponsor: Postdoctoral Science Foundation of China; contract grant number: 20090461108.
Contract grant sponsor: National Basic Research Program of China (973 Program); contract grant number: 2007CB209703.
Contract grant sponsor: National Natural Science Foundation of China; contract grant number: 20633040 and 20873064.

behaviors.[1] However, the problem of their degradation during cycling has to be solved. It has been already reported that composites based on carbon and conducting polymers, such as polypyrrole and polyaniline, are very interesting electrode materials for such supercapacitor applications.[24–26] Among the conducting polymers, poly(3,4-ethylene dioxythiophene) (PEDOT), a derivative of polythiophene, has been paid more attention. PEDOT presents a moderate value of the theoretical specific capacitance (210 F/g) because of its relatively high molar mass. Because of its moderate band gap, unique structural properties, and reaction mechanism, PEDOT has several advantages, such as a high transparency in the visible regime, excellent environmental stability, a wider potential window, suitable morphology, and high conductivity in a doped state (n or p type).[27,28] The stability of PEDOT in the oxidized form, its high conductivity, and its interesting electrochemical behavior allow this material to be used as an electrode in electrochemical capacitors. Therefore, PEDOT and its composites as electrode materials have been investigated for supercapacitors.[29–32] However, the long-term stability of PEDOT, similar to all other conducting polymers, could be a serious problem because of the typical shrinkage, breaking, and cracks appearing in subsequent cycles that are connected with volumetric changes of the polymer during the intercalation/deintercalation of counter ions. Thus, the combination of GO and PEDOT could be attractive for reinforcing the stability of PEDOT and for maximizing the capacitance value. To the best of our knowledge, the capacitor behavior of GO/PEDOT composites (GPTs) has not been reported so far.

In this study, PSS, the conventional dopant of PEDOT, which could circumvent the low solubility of 3,4-ethyldioxythiophene (EDOT), was used in the preparation of PEDOT and GPTs. GPTs were synthesized by a very facile *in situ* polymerization method in aqueous media. The electrochemical performances of GO, PEDOT–PSS, and GPT electrodes for supercapacitors were investigated. The composite electrode materials were expected to greatly improve the performances of the supercapacitors and to lead to a higher energy and power capability for various applications.

EXPERIMENTAL

Materials

GO was synthesized from natural graphite (325 mesh), which was kindly supplied Shandong Pingdu Graphite Co. (Qingdao, China). EDOT (Aldrich, Germany) was purified by distillation under reduced pressure and stored in a refrigerator before use. The oxidant ammonium persulfate (APS) was analytical grade and was purchased from Shanghai Lingfeng Chemical Reagent Co. (Shanghai, China). PSS (molecular weight = 80,000) was analytical grade and was obtained from Aldrich. All other reagents were analytical grade and were used as supplied without further purification.

Preparation of GO

GO was prepared by Hummer and Offeman's method.[33] Natural graphite powder was oxidized with $KMnO_4$ in concentrated H_2SO_4. Graphite powder (10 g) was added to 230 mL of cooled (0°C) H_2SO_4 (98%). $KMnO_4$ (30 g) and $NaNO_3$ (5 g) were added gradually with stirring and cooling to keep the temperature in the reactor at 10–15°C. The mixture was then stirred at 35°C for 30 min. Deionized water (250 mL) was slowly added to increase the temperature to 98°C, and the mixture was maintained at that temperature for 15 min. The reaction was terminated by the addition of 1 L of deionized water followed by 100 mL of a 5% H_2O_2 solution. The solid product was separated by centrifugation, washed repeatedly with a 5% HCl solution until sulfate could not be detected with $BaCl_2$, and then washed three to four times with acetone and dried in a vacuum oven at 60°C for 24 h.

Preparation of PEDOT–PSS

PSS (40 mg) was added to 20 mL of deionized water and sonicated to obtain a homogeneous PSS aqueous solution. EDOT monomer (110 μL, 1 mmol) was added dropwise to the previous solution and stirred for 20 min, and then, 2.5 mmol of APS was added in one portion. The polymerization was allowed to proceed overnight at room temperature. The product obtained was filtered and washed with deionized water and dried at 60°C for 24 h *in vacuo.*

Preparation of the GPTs

The GPTs were synthesized in a manner similar to an earlier work.[34] GO (100 mg) was added to 20 mL of PSS aqueous solution (40 mg of PSS dissolved in 20 mL of deionized water) and stirred for 4 h. The resulting colloidal solution of GO was then sonicated for 30 min. EDOT (110 μL, 1 mmol) and the oxidant APS (2.5 mmol) aqueous solution were added one after the other to the GO colloidal solution under vigorous stirring. The polymerization was allowed to proceed overnight at room temperature. The obtained product was filtered, washed with deionized water, and dried at 60°C for 24 h *in vacuo.*

Characterization

The morphological and structural characterization of GO, PEDOT–PSS, and the GPTs were analyzed by

Fourier transform infrared (FTIR) spectroscopy, scanning electron microscopy (SEM), and X-ray diffraction (XRD). The FTIR spectra were recorded from KBr pellets on a Bruker VECTOR22 FTIR spectrometer (USA). The SEM images were obtained with a Hitachi 4800 scanning electron microscope (Japan). The specimens were platinum-coated before examination. XRD patterns were obtained with a Rigaku D/MAX-RC X-ray diffractometer (Japan) with Cu Kα radiation. The electrical conductivity measurements were conducted on pressed pellets by the conventional four-probe technique at room temperature. The Brunauer–Emmett–Teller (BET) N_2 surface area and pore size distributions of the prepared composites were characterized with an Ominisorp 360 auto adsorption analyzer (Coulter, USA).

The electrochemical capacitive performances of GO, PEDOT–PSS, and the GPTs were evaluated separately with a three-electrode system. The working electrodes were fabricated by the mixture of electroactive materials (GO, PEDOT–PSS, GPTs), carbon black, and polytetrafluoroethylene in a mass ratio of 85 : 10 : 5 to make a homogeneous mixture. The resulting mixture was pressed onto a graphite current collector. The platinum foils and a saturated calomel electrode (SCE) were used as counter and reference electrodes, respectively. The electrolyte was 1*M* H_2SO_4. Cyclic voltammetry, galvanostatic charge–discharge, and electrochemical impedance spectroscopy were performed with a CHI660C electrochemical workstation (Shanghai Chenhua Instruments Company, Shanghai, China). Cyclic voltammetry tests were performed between −0.8 and 0.2 V at 10 mV/s. Galvanostatic charge–discharge curves were measured at a constant current density of 500 mA/g. Electrochemical impedance spectroscopy measurements were carried out in the frequency range from 10^5 to 0.01 Hz at open-circuit potential with an alternating-current perturbation of 5 mV. Galvanostatic cycling was performed between −0.2 and 0.8 V at a constant current density of 500 mA/g 1200 times with a LAND cell-testing system (Szland CT2001C, Wuhan, China) to evaluate the cycle stability.

RESULTS AND DISCUSSION

Figure 1 shows the FTIR spectra of GO, pristine PEDOT, PEDOT–PSS, and the GPTs. Figure 1(a) represents a typical IR spectrum of GO in accordance with the reported literature.[35] The band centered at 1720 cm^{-1} was associated with the stretching of the C=O bond of carbonyl or carboxyl groups. The bands centered at 1618 and 1384 cm^{-1} were attributed to deformations of the O—H bond in water and the CO—H groups, respectively. It was clear that the strong band ascribed to the C—H

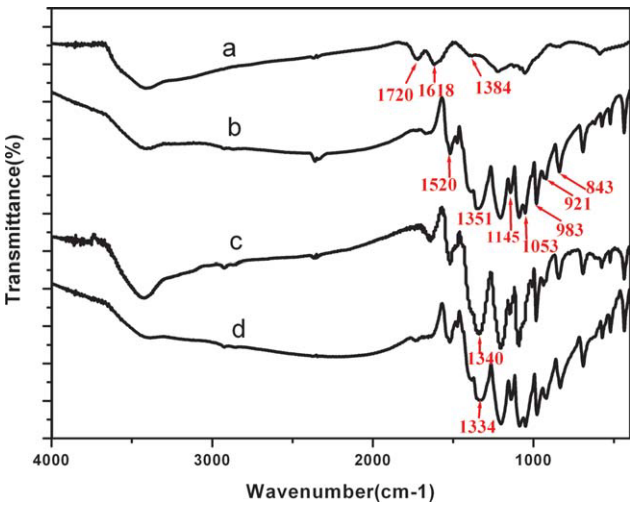

Figure 1 FTIR spectra of (a) GO; (b) pure PEDOT; (c) PEDOT-PSS; (d) GPTs. [Color figure can be viewed in the online issue, which is available at wileyonlinelibrary.com.]

bending mode at 891 cm^{-1} disappeared in the PEDOT bulk powder [pristine PEDOT; Fig. 1(b)] in comparison with the monomer spectrum; this demonstrated the formation of the PEDOT chains with α–α′ coupling. The vibrations around 1520 and 1351 cm^{-1} were attributed to the stretching modes of C=C and C—C in the thiophene ring.[36,37] The vibration modes of the C—S bond in the thiophene ring[36] were seen at 983 and 843 cm^{-1}. The bands at 1145 and 1053 cm^{-1} were assigned to the stretching modes of the ethylenedioxy group, and the band around 921 cm^{-1} was due to the ethylenedioxy ring deformation mode.[36,37] With the PEDOT bulk powder spectrum as a reference, the FTIR spectra of both PEDOT–PSS and the GPTs [Fig. 1(c,d)] showed the characteristic peaks of pristine PEDOT. The vibration band attributed to C—C stretching in the thiophene ring in PEDOT–PSS and the GPTs had a redshift from 1351 to 1340 and 1334 cm^{-1}. This was related to the electrostatic interaction between the EDOT cations and the PSS anions and the electronegative functional groups on the GO layers for the GPTs. GO bands were scarcely detectable in the GPT spectrum, probably because either they were too weak or they overlapped with the absorption peak of PEDOT.

The XRD patterns provided useful information about the *d*-spacing of GO and the GPTs when Bragg's law was followed at the peak positions:

$$d = n\lambda/(2\sin\theta)$$

where θ is the angle between the incident ray and the scattering planes, n is an integer determined by the order given, and λ is the wavelength. As shown in Figure 2, the XRD pattern of GO was different from that of the GPTs. Pristine GO had a layered structure with an interlayer spacing of 0.80 nm. This

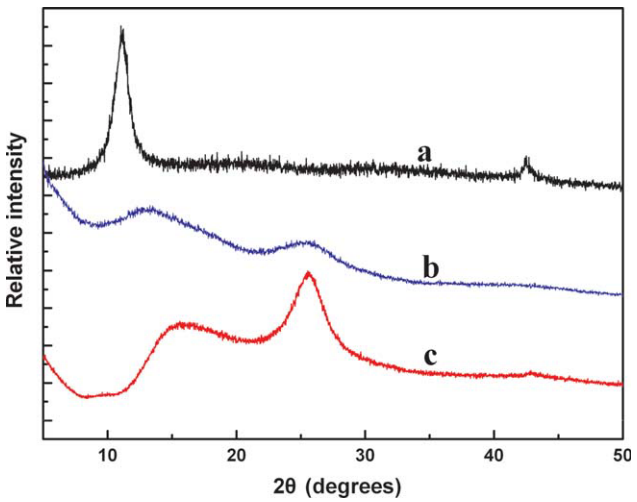

Figure 2 XRD patterns of (a) GO; (b) PEDOT-PSS; (c) GPTs. [Color figure can be viewed in the online issue, which is available at wileyonlinelibrary.com.]

suggested that there existed intercalated water in the layer of GO because the GO interlayer distance depended strongly on the GO:H_2O ratio.[38] As shown in Figure 2(b), two broad and diffused reflection peaks near $2\theta = 13$ and 25° were observed in the XRD pattern of PEDOT–PSS; these were attributed to PEDOT with an amorphous structure.[39] The XRD pattern of the GPTs showed an amorphous halo near $2\theta = 15.7°$. The halo was interpreted as scattering from the irregularly aggregated GO sheets.[40] This indicated that the polymerization of EDOT caused the partial delamination of the stacked GO plates. In such exfoliated composites, the incorporation of PEDOT into the GO provided a low resistance path within the electrode, and the existence of SO_3H groups in PSS generated a pathway for protonic species, which increased the ionic conductivity of the GPTs.[41] As a result, the electrochemical properties of the GPTs were promoted. In addition, the GPTs exhibited an intense diffraction peak at about $2\theta = 25.6°$ (i.e., $d = 0.35$ nm); this indicated some crystalline order of PEDOT in the GPTs.

SEM images of GO, PEDOT–PSS, and the GPTs at different magnifications are presented in Figure 3. Figure 3(A,a) shows that a considerable number of

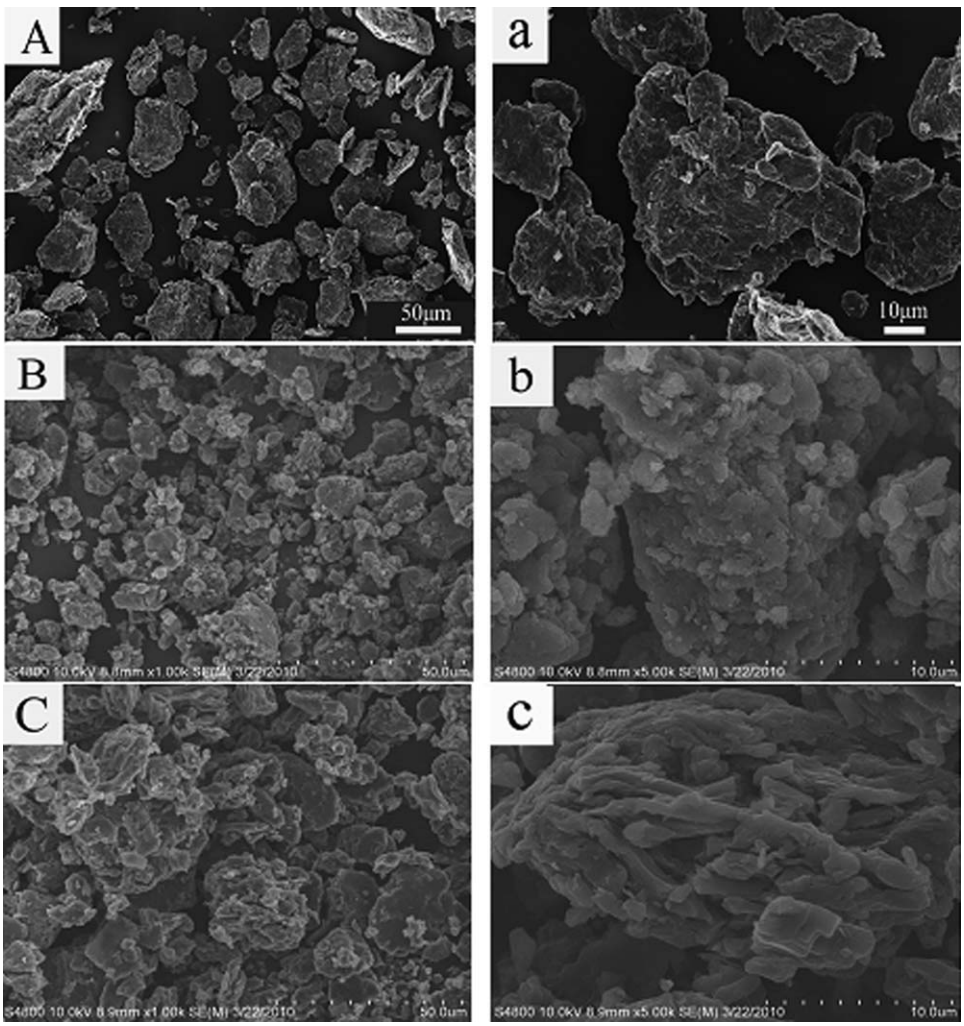

Figure 3 SEM images of (A,a) GO, (B,b) PEDOT–PSS, and (C,c) GPTs.

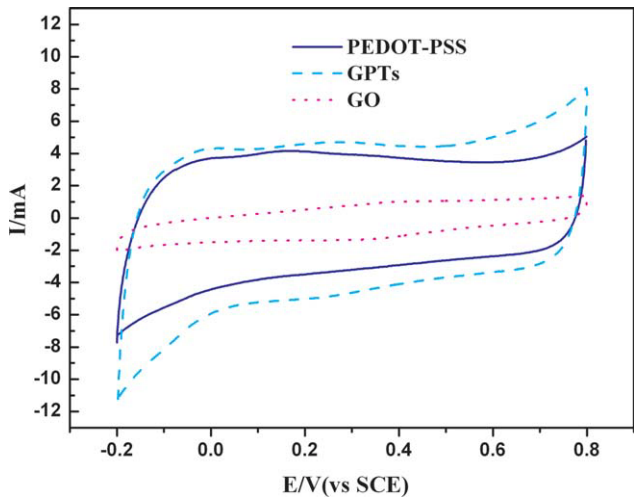

Figure 4 (E = potential, I = current). Cyclic voltammograms of GO; PEDOT-PSS and GPTs in 1M H_2SO_4 at 10 mV/s. [Color figure can be viewed in the online issue, which is available at wileyonlinelibrary.com.]

GO layers overlapped tightly together in an irregular form with the size of 10s of micrometers. PEDOT–PSS showed the typical morphology of submicrometer- or micrometer-sized layered structures stacked on each other. A significant change in the morphology [Fig. 3(C,c)] was observed when EDOT was polymerized in the presence of GO. As shown in Figure 3(c), the GO layers were partially delaminated into individual micrometer-sized GO layers in the GPTs; this was in agreement with the results of the XRD patterns. The surface of GO became fluffy [Fig. 3(C)] because of the incorporation of PEDOT–PSS and formed layer-on/within-layer composite structure. Such a special structure might have led to more sites that were susceptible to redox reactions, a greater active area, and consequently, higher capacitance.

The cyclic voltammograms of GO, PEDOT–PSS, and the GPTs, with a potential window from −0.2 to 0.8 V (vs SCE), are shown in Figure 4, and the representative charge/discharge curves at a current density of 500 mA/g are shown in Figure 5. The specific capacitance (C_m) of the samples were estimated from the discharge process according to the following equation:

$$C_m = \frac{C}{m} = \frac{I\Delta t}{m\Delta v} \quad (1)$$

where C is capacitance, I is the discharge current, Δt is the discharge time, m is the mass of the active material, and Δv is the potential drop in the discharge progress.

The cyclic voltammetry curve of GO showed a small deviation from an ideal rectangular shape; this indicated good charge propagation within the electrode. However, the C_m value calculated from the discharge process shown in Figure 5(a) was only 11 F/g, probably because of the low conductivity of GO prepared here (1×10^{-5} S/cm). The functional groups on the GO layers should have made the electron pathway discontinuous during the charge and delivery processes. As shown in Figure 4(b,c), the curves of PEDOT–PSS and the GPTs displayed rectangle-like shapes; this showed a very fast electrochemical switch. The output currents of PEDOT–PSS and the GPTs were much larger than that of pristine GO. Because capacitance can be estimated from the output current divided by the scan rate, this indicated that the specific capacitances of

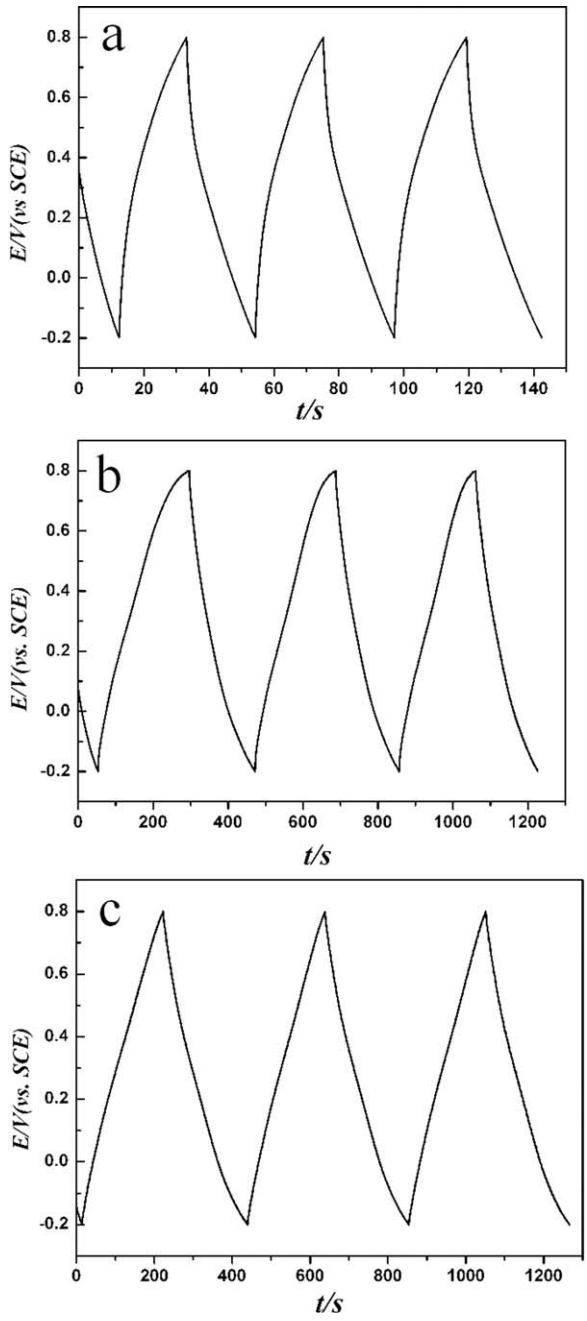

Figure 5 Galvanostatic charge–discharge curves of (a) GO, (b) PEDOT–PSS, and (c) GPTs at a constant current density of 500 mA/g (E = potential, t = time).

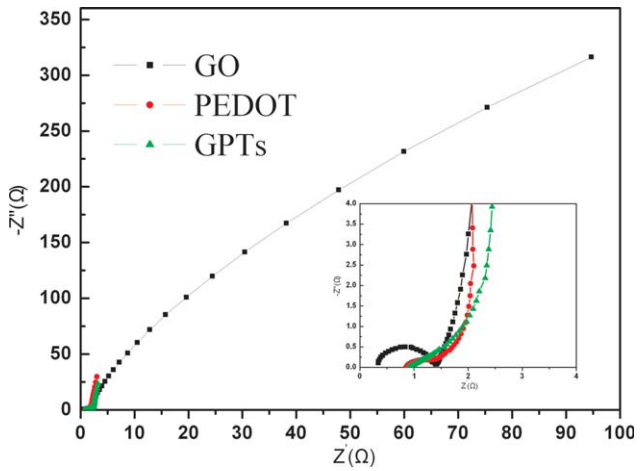

Figure 6 The specific capacitance change of PEDOT-PSS and GPTs at a constant current density of 500mA/g as a function of cycle number. (Z′ = realistic impedance, Z″ = imaginary part of the impedance test.) [Color figure can be viewed in the online issue, which is available at wileyonlinelibrary.com.]

PEDOT–PSS and the GPTs were larger than that of GO. This improvement may have been due to the high surface area and good conductivity of PEDOT–PSS (1.4 S/cm) and the GPTs (1.0 S/cm). The accurate C_m values obtained from the discharge process in Figure 5(b,c) were 87 and 108 F/g for PEDOT–PSS and GPTs, respectively. When EDOT was polymerized in the presence of GO, the obtained GPTs retained the most facile pathways for both electron and proton conduction and had the best utilization compared to both GO and PEDOT–PSS; this resulted in the high specific capacitance. As a result, the specific capacitance of the resultant GPTs (108 F/g) was correspondingly promoted and was even higher than the sum specific capacitances of GO (11 F/g) and PEDOT–PSS(87 F/g); this may have been a synergistic effect of the pristine component. It is known that the BET surface area is directly correlated to EDLC. The BET (N_2) specific surface area of the GPTs was 19 m^2/g. Calculation of the pure EDLC with the BET (N_2) specific surface area of an average value of 20 $\mu F/cm^2$ gave an EDLC value of about 3.8 F/g for the GPTs, which was much lower than the corresponding measured C_m of 108 F/g.[42] Therefore, it was demonstrated that the main component of the measured C_m was produced from the pseudocapacitive surface redox process. In addition, for the GPTs, when the current density was increased to 2 A/g, the specific capacitance still remained at a high level of 88 F/g without a significant decrease in the charge–discharge cycling.

Typical Nyquist plots of GO, PEDOT–PSS, and GPT electrodes are given in Figure 6. The presence of the semicircles indicates an obvious resistance for electron conduction in the GO electrode.[43,44] This may have been due to the presence of functional groups to hinder electron conduction between the GO aggregates. For the case of PEDOT–PSS and the GPTs, a semicircle at high frequency was not detected; this indicated that interfacial charge-transfer resistance among them was significantly low because of their high conductivity. At low frequency, the impedance plots of PEDOT–PSS and the GPTs exhibited a slightly tilted vertical line of a limiting diffusion process in the electrolyte of 1*M* H_2SO_4; this is a characteristic feature of pure capacitive behavior.

The cycle-life tests of PEDOT–PSS and the GPTs as supercapacitor electrodes were carried out after sequential charge–discharge cycling at a constant current density of 500 mA/g. As is obvious in Figure 7, the loss of specific capacitance for PEDOT–PSS was larger; a capacitance retention of about 66% was found over 1200 cycles. In contrast, the loss of specific capacitance for the GPT electrode was smaller and showed a stable cycle life; a capacitance retention of about 78% was found over 1200 cycles. These data suggested that the presence of GO sheets in the GPTs improved the cycling stability of the supercapacitors, likely because of the constructed layer-on/within-layer composite structure of the GPTs. Such a low decrease in the specific capacitance after a long time of operation indicated the high stability of the composites and their potential as electrode materials for long-term capacitor applications.

CONCLUSIONS

In this study, GPTs for electrochemical electrodes were fabricated, and their performance for supercapacitor electrodes was investigated. The incorporation of PEDOT in the GPTs led to an improved electrical conductivity, and this resulted in a high

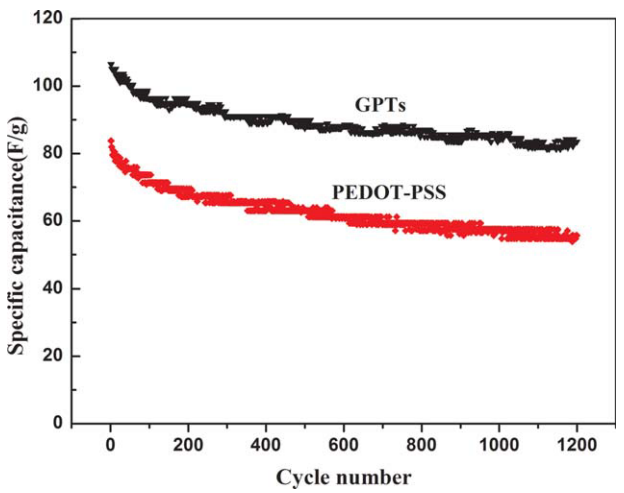

Figure 7 The specific capacitance change of PEDOT-PSS and GPTs at a constant current density of 500mA/g as a function of cycle number. [Color figure can be viewed in the online issue, which is available at wileyonlinelibrary.com.]

specific capacitance. The specific capacitance of the GPTs was found to be as high as 108 F/g at a constant current density of 500 mA/g; this was even higher than the sum of the specific capacitances of pristine GO (11 F/g) and PEDOT–PSS (87 F/g). Moreover, the presence of partially exfoliated GO sheets in the GPTs improved the cycling stability of the supercapacitors, likely because of the constructed layer-on/within-layer composite structure of the GPTs. The loss of the specific capacitance for the GPT electrode was smaller and showed a stable cycle life; a capacitance retention of about 78% was found over 1200 cycles. Our study suggests that GPTs have promising electrochemical properties for applications as supercapacitor electrodes.

References

1. Conway, B. E. Electrochemical Supercapacitors, Scientific Fundamentals and Technological Application; Kluwer Academic: New York, 1999.
2. Conway, B. E. J Electrochem Soc 1991, 138, 1539.
3. Burke, A. J Power Sources 2000, 91, 37.
4. Simon, P.; Gogotsi, Y. Nat Mater 2008, 7, 845.
5. Pandolofo, A. G.; Hollenkamp, A. F. J Power Sources 2008, 157, 11.
6. Carbon Nanomaterials; Gogotsi, Y., Ed.; CRC: Boca Raton, FL, 2006.
7. Portet, C.; Chmiola, J.; Gogotsi, Y.; Park, S.; Lian, K. Electrochim Acta 2008, 53, 675.
8. Yang, C. M. J Am Chem Soc 2007, 129, 20.
9. Patake, V. D.; Pawar, S. M.; Shinde, V. R.; Gujar, T. P.; Lokhande, C. D. Curr Appl Phys 2010, 10, 99.
10. Ragupathy, P.; Park, D. H.; Campet, G.; Vasan, H. N.; Hwang, S. J.; Choy, J. H.; Munichandraiah, N. J Phys Chem C 2009, 113, 6303.
11. Patake, V. D.; Lokhande, C. D.; Joo, O. S. Appl Surf Sci 2009, 255, 4192.
12. Patake, V. D.; Lokhande, C. D. Appl Surf Sci 2008, 254, 2820.
13. Lee, S.; Cho, M. S.; Nam, J. D.; Lee, Y. J Nanosci Nanotechnol 2008, 8, 5036.
14. Amarnath, C. A.; Chang, J. H.; Kim, D.; Mane, R. S.; Han, S. H.; Sohn, D. Mater Chem Phys 2009, 113, 14.
15. Zang, J. F.; Bao, S. J.; Li, C. M.; Bian, H. J.; Cui, X. Q.; Bao, Q. L.; Sun, C. Q.; Guo, J.; Lian, K. R. J Phys Chem C 2008, 112, 14843.
16. Ismail, Y. A.; Chang, J.; Shin, S. R.; Mane, R. S.; Han, S. H.; Kim, S. J. J Electrochem Soc A 2009, 156, 313.
17. He, H.; Klinowski, J.; Forster, M.; Lerf, A. Chem Phys Lett 1998, 287, 53.
18. Lerf, A.; He, H.; Riedl, T.; Forster, M.; Klinowski, J. Solid State Ionics 1997, 101, 857.
19. Lerf, A.; He, H.; Forster, M.; Klinowski, J. J Phys Chem B 1998, 102, 4477.
20. Hontoria-Lucas, C.; Lopez-Peinado, A. J.; Lopez-Gonzalez, J. D.; Rojas-Cervantes, M. L.; Martin-Aranda, R. M. Carbon 1995, 33, 1585.
21. Yang, S.; Kim, I. J.; Jeon, M. J.; Kim, K.; Moon, S. I.; Kim, H. S.; An, K. H. J Ind Eng Chem 2008, 14, 365.
22. Jeong, H. K.; Jin, M.; Ra, E. J.; Sheem, K. Y.; Han, G. H.; Arepalli, S.; Lee, Y. H. ACS Nano 2010, 4, 1162.
23. Tien, C. P.; Teng, H. J Power Sources 2010, 195, 2414.
24. Muthulakshmi, B.; Kalpana, D.; Pitchumani, S.; Renganathan, N. G. J Power Sources 2006, 158, 1533.
25. Kim, J. H.; Lee, Y. S.; Sharma, A. K.; Liu, C. G. Electrochim Acta 2006, 52, 1727.
26. Zhou, Y.; Qin, Z. Y.; Li, L.; Zhang, Y.; Wei, Y. L.; Wang, L. F.; Zhu, M. F. Electrochim Acta 2010, 55, 3904.
27. Pei, Q.; Zuccarello, G.; Ahlskog, M.; Inganas, O. Polymer 1994, 35, 1347.
28. Groenendaal, L.; Jonas, G.; Freitag, D.; Pielartzik, H.; Reynolds, J. R. Adv Mater 2000, 12, 481.
29. Patra, S.; Munichandraiah, N. J Appl Polym Sci 2007, 106, 1160.
30. Ryu, K. S.; Lee, Y. G.; Hong, Y. S.; Park, Y. J.; Wu, X. L.; Kim, K. M.; Kang, M. G, Park, N. G. Electrochim Acta 2004, 50, 843.
31. Liu, K. K.; Hu, Z. L.; Xue, R.; Zhang, L.; Zhu, J. J. J Power Sources 2008, 179, 858.
32. Sharma, R. K.; Zhai, L. Electrochim Acta 2009, 54, 7148.
33. Hummers, W. S.; Offeman, R. E. J Am Chem Soc 1958, 80, 1339.
34. Han, Y. Q.; Lu, Y. Compos Sci Technol 2009, 69, 1231.
35. Titelman, G. I.; Gelman, V.; Bron, S.; Khalfin, R. L.; Cohen, Y.; Bianco-Peled, H. Carbon 2005, 43, 641.
36. Kvarnström, C.; Neugebauer, H.; Blomquist, S.; Ahonen, H. J.; Kankare, J.; Ivaska, A. Electrochim Acta 1999, 44, 2739.
37. Garreau, S.; Louarn, G.; Buisson, J. P.; Froyer, G.; Lefrant, S. Macromolecules 1999, 32, 6807.
38. Kovtyukhova, N. I.; Ollivier, P. J.; Martin, B. R.; Mallouk, T. E.; Chizhik, S. A.; Buzaneva, E. V.; Gorchinskiy, A. D. Chem Mater 1999, 3, 771.
39. Niua, L.; Kvarnström, C.; Fröbergb, K.; Ivaska, A. Synth Met 2001, 122, 425.
40. Sasaki, T.; Watanable, M. J Am Chem Soc 2000, 77, 2201.
41. Kuo, C. W.; Huang, L. M.; Wen, T. C.; Gopalan, A. J Power Sources 2006, 160, 65.
42. Cao, L.; Lu, M.; Li, H. L. J Electrochem Soc A 2005, 5, 871.
43. Nian, J. N.; Teng, H. J Phys Chem B 2005, 109, 10279.
44. Huang, C. W.; Chuang, C. M.; Ting, J. M.; Teng, H. J Power Sources 2008, 183, 406.